JOURNAL OF COLLOID AND INTERFACE SCIENCE **203,** 369–378 (1998)
ARTICLE NO. CS985541

Analysis of Bacterial Deposition on Metal (Hydr)oxide-Coated Sand Filter Media

S. E. Truesdail,* J. Lukasik,† S. R. Farrah,† D. O. Shah,* and R. B. Dickinson*,[1]

*Department of Chemical Engineering and †Department of Microbiology and Cell Science, University of Florida, Gainesville, Florida 32611-6005

Received September 30, 1997; revised March 18, 1998

The aim of this study was to investigate the importance of surface potential in microbial deposition onto modified granular surfaces. Recent experimental and theoretical work has indicated that surfaces coated with metal oxides and hydroxide rich oxide/hydroxide mixtures ((hydr)oxides) have the potential to increase the capture efficiencies of commercial filtration systems. This study quantitatively compared different metal (hydr)oxide coatings in their abilities to enhance bacterial deposition. Specifically, the deposition rates of bacterial strains *Streptococcus faecalis, Staphylococcus aureus, Salmonella typhimurium,* **and** *Escherichia coli* **were compared for Ottawa sand and surface coatings consisting of aluminum (hydr)oxide, iron (hydr)oxide, and mixed iron and aluminum (hydr)oxide. The metal-(hydr)oxide-modified granular media enhanced bacterial deposition relative to the noncoated Ottawa sand. The electropositive surfaces, the aluminum and the mixed (hydr)oxides, had similar average kinetic rate constants, five times larger than the rate constants observed for the untreated Ottawa sand. The measured kinetic rate constants for the positively charged systems of aluminum (hydr)oxide and mixed (hydr)oxide collectors suggested that the overall rate of deposition was limited by the transport of bacteria to the granular surface rather than the rate of attachment. For systems where the collector surfaces were negatively charged, as in the cases of Ottawa sand and the iron (hydr)oxide coating, large energy barriers to attachment were predicted from DLVO theory but these barriers did not totally inhibit bacterial deposition. The deposition results could not be fully explained by DLVO theory and suggested the importance of other factors such as collector charge heterogeneity, motility, and bacterial surface appendages in enhanced deposition.**

Key Words: **metal hydroxides; DLVO theory; bacterial deposition; granular media; charge heterogeneity.**

1. INTRODUCTION

There has recently been a concerted effort toward improving microbial removal efficiencies of industrial and municipal filtration processes through the modification of filtration media. Several recent papers have described enhanced removal efficiencies in filtration systems utilizing metal oxides and metal hydroxides (1–5). In spite of some success in this area, a fundamental understanding of why deposition is improved to a greater degree in some coatings and not in others often appears to be lacking. Improved understanding of the mechanisms influencing particle attachment could aid in the design of more efficient filter media in a wide range of industrial applications. Bacterial adhesion, however, is difficult to quantify at a fundamental level. Hydration forces (6), hydrophobic interactions (8–11), macromolecular bridging (12), surface roughness (13), and electrical double-layer and van der Waals forces (1, 7, 14–16) have all been proposed as possible influences on adhesion. Many of these factors, however, are difficult to experimentally measure for microbial attachment to granular media. An arguable exception to this observation is the measurement of zeta potential and its influence on particle interaction forces. This study attempts to exploit these electrical double-layer and van der Waals forces with the use of metal hydroxide coatings in order to improve microbial adhesion.

The role of electrical double-layer and van der Waals forces in particle deposition is often viewed in terms of DLVO theory (17, 18). Figure 1 illustrates two regions of particle deposition predicted by DLVO theory for the interaction between two charged surfaces. The dashed line represents the interaction expected between a strong negatively charged collector such as Ottawa sand and a negative bacteria particle. This line falls in a region where the rate of particle attachment to the surface is controlled by double-layer repulsive forces and the resulting interaction energy barrier. As the magnitude of these like charges on the interacting particles decreases the DLVO theory predicts the van der Waals force to dominate at short separation distances. This eventually results in a finite energy barrier around 10 kT where the particle attachment event (controlled by the energy barrier) no longer determines particle capture (solid center line). For an oppositely charged collector and particle, the energy barrier disappears such that the rate of deposition is controlled by the rate of diffusion or convective transport of bacteria to the surface (19). Alteration of the surface potential of the granular collector medium to be posi-

[1] To whom correspondence should be addressed (fax: (352) 392-9513; e-mail: dickinso@che.ufl.edu).

0021-9797/98 $25.00

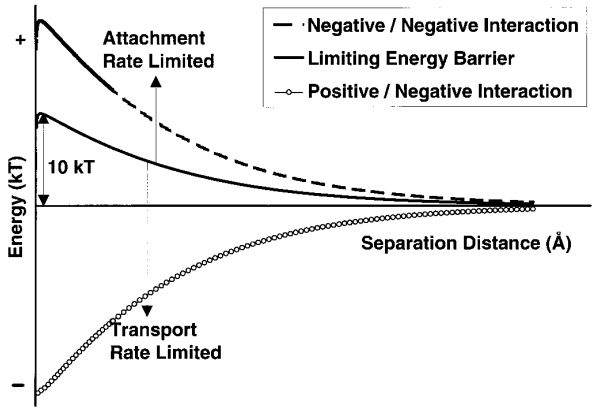

FIG. 1. Set of hypothetical Helmholtz potential energy curves illustrating the expected interaction energies for oppositely charged particles (lower line), and similarly charged particles with increasingly larger charge magnitudes (upper dashed line). The solid center line represents the boundary between attachment rate limited deposition and transport limited particle deposition.

tive, as observed for the metal-hydroxide-rich coatings used within this study, removes the repulsive double-layer interaction. Two oppositely charged surfaces should therefore experience stronger attraction over greater separation distances (1). This favorable interaction is shown in Fig. 1 as the lower line and represents a case in which the kinetic rate constants of deposition should be controlled by particle transport to the collector surface. Most bacteria are negatively charged because of the predominance of the anionic groups present within the cell wall (carboxyl, amino, and phosphate groups); therefore, a positively charged collector surface should enhance particle deposition. Metal hydroxides were chosen for this study over metal oxides because of the experimental and theoretical observation that the hydroxides tended to provide a more positively charged surface (20, 21).

In this study, bacterial deposition kinetics were measured for precipitated coatings rich in metal hydroxides to investigate the role of DLVO forces (electrical double-layer and van der Waals forces) in filtration. The surfaces examined were Ottawa sand, aluminum (hydr)oxide coated Ottawa sand, iron (hydr)oxide coated Ottawa sand, and mixed iron–aluminum (hydr)oxide coated Ottawa sand. Rates of microbial deposition were compared for these different granular media and bacterial strains *Streptococcus faecalis*, *Staphylococcus aureus*, *Salmonella typhimurium*, and *Escherichia coli*. Through the analysis of deposition results, the influence of surface potential of the metal (hydr)oxide coatings on bacterial deposition will be determined within systems of granular media.

2. MATERIALS AND METHODS

2.1. Granular Surface Preparation

The coating procedure of the Ottawa sand has been described elsewhere (5) and is summarized here. Ottawa sand (20–30 mesh) was soaked in 1 M ferric chloride or 1 M aluminum chloride solution for 30 min (all materials obtained from Fisher, Fairlawn, NJ). The excess solution was drained and the sand was allowed to dry. The sand was then soaked in 2 volumes of 3 M ammonium hydroxide for 10 min, drained and again air dried. The mixed coating was created through simultaneous treatment of the sand with the 0.25 M $FeCl_3$ and 0.5 M $AlCl_3$ and was subjected to similar washing and drying procedures. The following reactions were expected for these systems:

$$AlCl_3 + 3NH_4(OH) \rightarrow Al(OH)_3 + 3NH_4Cl$$

$$FeCl_3 + 3NH_4(OH) \rightarrow FeO(OH) + 3NH_4Cl + H_2O.$$

The actual crystal structures produced in these reactions were expected to contain the polymorphs of $FeO(OH)$ and $Al(OH)_3$ and possibly some of the respective oxides. It is for this reason that the term (hydr)oxides has been employed to describe the metallic precipitated surfaces. Again, the dominance of the metal hydroxide polymorphs in the coating is expected to reduce the double-layer repulsion between the bacteria and the coated collectors relative to the unmodified SiO_2 (Ottawa sand).

All samples were subjected to preattritioning on a vertical 70-cm diameter spinning wheel at 30 rev/min for 30 min to remove any loosely adhered surface precipitates. These weakly adhered particles of metallic coating were removed to ensure the validity of the batch deposition studies by eliminating additional microorganism removal through mechanisms involving the settling of bacteria/metal (hydr)oxide flocs. Coating solubility was predicted not to be a significant factor in these studies because of the relatively low solubility of the aluminum ($10^{-6.4}$ M) and iron species ($10^{-11.4}$ M) (22).

2.2. Granular Surface Characterization

The zeta potential of the granular collector medium was determined using a streaming potential apparatus. The apparatus consisted of a flow-through sample cell that was packed with the granular medium to be analyzed and a tank to supply electrolyte. A water manometer monitored the pressure drop across the cell and a Keithly 610c electrometer was used to measure the electrical potential between two silver chloride electrodes which preceded and followed the granular sample. Sand samples were uniformly packed into the sample cell via the tap and fill methodology. The sample cell was then flushed with carbon dioxide and then the KCl electrolyte solution to remove any potential air pockets. The actual physical operation of the streaming potential device consisted of flowing a 1.0×10^{-4} M KCl salt solution through the granular sample under investigation. Pressure was used as the controlled variable in these measurements and was allowed to range over the entire laminar flow regime as

determined from the Reynolds and Burk–Plummer equations (23). Electrodes at the edges of the sample monitored the voltage generated as the charged ions in the KCl solution passed the charged sample surface under investigation. This voltage varied as a function of pressure drop. The slope of the plotted voltage and pressure values was then used along with the measured solution conductivity to calculate the corresponding zeta potential with the equation (24)

$$\zeta = \frac{4\pi\mu K}{\epsilon\epsilon_0}\frac{\Delta E}{\Delta P}, \qquad [1]$$

where ζ represents the zeta potential, μ the viscosity of the electrolyte solution, K the solution conductivity, ϵ the dielectric constant of the electrolyte, ϵ_0 the dielectric constant of a vacuum, E the electromotive potential, and P the pressure across the packed bed. Because of the weak electrolytic nature of the solution used in these measurements, the zeta potential was assumed to be very close to the surface potential and was the value used in the DLVO calculations. The above-mentioned methodology has accurately reproduced zeta measurements for multiple samples given in the literature and was found to provide a reproducibility within $\pm 10\%$ of the measured zeta potential. This error value was based upon the 95% confidence interval for the solution conductivity and the pressure–voltage slope variables used in Eq. [1].

Inductively coupled plasma spectroscopy (ICP) was run to quantify the concentration of iron and aluminum present on the collector's surface for both modified and unmodified Ottawa sand. A quantity of 10 g of collector material was digested in 25 ml of aqua regia (1:2:2::HCl:HNO_3:H2O) for 20 min. The solution was heated to a near boil, diluted to 1000 ml, and filtered through a 0.2-micron pore-size filter prior to ICP analysis. The pH of the dilute solution should be relatively neutral in order to prevent damage to the ICP instrumentation. The diluted samples were then run in triplicate for all four collector surfaces before and after the deposition experiments to test for the loss of iron and aluminum.

Surface area measurements were performed with a Quantachrome NOVA 1200 apparatus. Because of the rather large sizes of the studied granular media ($\sim$0.7-mm diameter) a large calibrated cell capable of holding around 8 g of granular material was used in an 11-point BET adsorption analysis. Specific surface areas were based upon four repeated measurements and a correlation coefficient generally greater than 0.99.

Energy dispersive spectroscopy (EDS) was used to probe the silica surface for elemental impurities. In addition, scanning electron microscope elemental microprobe (SEMEM) analysis was used to examine the relative surface density and uniformity of the metal species on all four of the collector surfaces. The technique also allowed for an estimation of the charge heterogeneity on each surface.

2.3. Bacteria Preparation

Streptococcus faecalis (ATCC 19433), *Staphylococcus aureus* (ATCC 12600), *Salmonella typhimurium* (ATCC 19585), and *Escherichia coli* C3000 (ATCC 15597) were each grown in 3% tryptic soy broth overnight at 37°C. The *E. coli* and *S. typhimurium* were cylindrical, motile, gram-negative strains, whereas *S. aureus* and *S. faecalis* were spherical, nonmotile, and gram-positive. The bacterial suspensions were individually centrifuged, rinsed, and resuspended in distilled water two times before zeta potential and deposition experiments. All bacteria/distilled water samples were used within 1 h of preparation and no osmotic lysis was observed.

2.4. Bacterial Surface Potential

The zeta potential measurements for these bacteria were carried out with the use of a Brookhaven Instrument's Zetaplus model v3.21 zeta potential analyzer (Holtsville, NY). Each sample was pre-rinsed as previously stated and further diluted to a final concentration of 1.0×10^7 CFU/ml with pH-controlled distilled water. Distilled water was chosen to minimize any charge shielding within the electrical double layer. Experimental measurements of zeta potentials utilizing ionic and organic buffers resulted in the invalidation of the assumed equality between the measured zeta potential and the surface potential. In addition, surface conduction within the microbe lipid membranes may have resulted in some degree of underrepresentation of the microbe's zeta potentials during the conversion from electrophoretic mobilities via the Helmholtz–Smoluchowski equation (25).

2.5. Deposition Measurement

The deposition studies of the four selected bacteria were carried out under batch conditions at 25°C. The pH was manipulated to 7.0 with weak KOH solution and the resulting electrolyte concentration was calculated to be 1.1×10^{-5} M. An 8 ml volume of $\sim 10^5$ CFU/ml bacteria solution at pH 7.0 was then added to a number of presterilized polypropylene 50-ml conical tubes each having 5 g of sand. The samples were then placed horizontally onto a New Brunswick orbital shaker table and gently agitated at a speed of 120 rounds per minute. The supernatant was sampled at various times and diluted 10-fold in tryptic soy broth (DIFCO Laboratory Inc., Detroit, MI) before spread plating. The bacterial deposition was determined through plating and the comparison between the number of culture forming units observed for the supernatant at time (t) with the bacterial number observed for the control samples (C_0). Bacterial deposition due to contact with the polypropylene walls of the conical tubes was assumed negligible as confirmed through deposition measurements in the absence of granular media.

2.6. Modeling Deposition Data to Determine the Kinetic Rate of Particle Attachment

To quantify this rate of particle attachment from the experimental deposition studies, a first-order kinetic model was used to the fit the data. It was initially assumed that the adsorption process observed within these deposition studies could be described by a first-order kinetic rate constant (k) that was taken to be invariable with respect to time and uniform among the bacteria population. This would imply the rate change of bacteria in the supernatant to be

$$\frac{dC}{dt} = -kC, \qquad [2]$$

where C represents the concentration of bacteria remaining in the supernatant. In relation to the initial bacterial concentration, C_0, Eq. [2] was then solved to produce

$$C(t) = C_0 e^{-kt}. \qquad [3]$$

Equation [3] was fitted to the experimental data using nonlinear regression to estimate fitted parameters C_0 and k.

2.7. DLVO Calculations

The theoretical potential energy of interaction, E_{DLVO}, between the bacteria and collector was calculated using DLVO theory. A granular collector and bacterium were modeled as a flat plate and sphere, respectively, such that E_{DLVO} can be written as (6)

$$E_{DLVO} = E_{vdw} + E_{double}, \qquad [4]$$

where E_{vdw} is the interaction potential due to van der Waals forces, and E_{double} is the interaction potential due to double-layer forces. The van der Waals term (E_{vdw}) was determined by (7)

TABLE 1
Bacterial Properties Used in the Calculation of the DLVO Energy Curves

Bacterium	Diameter	(95% CI)	Zeta potential (pH = 7.0)	Zeta potential (95% CI)
E. coli	8.82×10^{-7} m[a]	$\pm 2.8 \times 10^{-8}$ m	−36.5 mV	± 2 mV
S. typhimurium	8.73×10^{-7} m[a]	$\pm 4.0 \times 10^{-8}$ m	−17 mV	± 1 mV
S. aureus	5.89×10^{-7} m	$\pm 9.0 \times 10^{-9}$ m	−36 mV	± 1 mV
S. faecalis	6.39×10^{-7} m	$\pm 1.3 \times 10^{-8}$ m	−38.5 mV	± 1.5 mV

[a] Equivalent surface spherical diameters.

TABLE 2
Values Used in the Calculation of the Hamaker Constant (6)

Material	Dielectric constant	Refractive index
Ottawa sand[a]	3.8	1.448
Al_2O_3	11.6	1.75
Fe_3O_4	14.2	1.97
Al_2O_3/Fe_3O_4 mix	12.45	1.82
H_2O	78.54	1.333
Bacteria	78.54	1.55

[a] Taken as quartz.

$$E_{vdw} = \frac{-A_{123}}{6}\left[\frac{a}{h} + \frac{a}{h+2a} + \ln\left(\frac{h}{h+2a}\right)\right], \qquad [5]$$

where A_{123} is the nonretarded Hamaker constant for the system (1, collector; 2, water; 3, bacteria), a is the radius of the bacteria, and h is surface-to-surface separation distance between the collector and the bacterium. The diameters of the spherical bacteria and equivalent surface spherical dimensions of the cylindrical bacteria were determined with the aid of UTHSCSA version 1.1 image analysis software and multiple SEM micrographs (Table 1). In the determination of the van der Waals component of the energy, the Hamaker constant (A_{123}) was calculated with standard nonretarded Lifshitz theory (6) for the various surfaces and bacterial combinations. Literature values were used for the dielectric constants and refractive indices of the granular surface coatings (Table 2). A dielectric constant of 78.54, a number reflecting the fact that the bacteria were primarily composed of water, was also assumed for the calculation. (The error associated with this assumption was expected to be very small because of the relative insensitivity of the Hamaker calculation to changes within the dielectric constant.) The bacterial refractive index has been reported to lie within the range of 1.5 to 1.6 (6) and a value of 1.55 was used to represent each of the four bacteria in the Hamaker constant calculations (Table 3).

TABLE 3
Granular Collector Surface Properties and Respective Hamaker Values

Granular surface	Surface potential (pH 7.0)	Surface potential (95% C.I.)	Hamaker constant	Surface area
Mixed (hydr)oxide	+35 mV	±2 mV	2.53×10^{-20}	0.35 m^2/g
Iron (hydr)oxide	−50 mV	±2 mV	3.22×10^{-20}	0.32 m^2/g
Aluminum (hydr)oxide	+22 mV	±3 mV	2.20×10^{-20}	0.26 m^2/g
Ottawa sand	−90 mV	±6 mV	6.60×10^{-21}	0.46 m^2/g

Note. Hamaker constant values were within the expected ranges typically predicted for the corresponding oxide surfaces, 1.7 to 4.2 $\times 10^{-20}$ (36).

The double-layer potential was given by an adapted Wiese and Healy expression for a sphere–flat plate system (7),

$$E_{\text{double}} = 2\pi a n_\infty k_B T \frac{\varphi_1^2 + \varphi_2^2}{\kappa^2}\left[\frac{2\varphi_1\varphi_2}{\varphi_1^2 + \varphi_2^2} \times \ln\left(\frac{1 + e^{-\kappa h}}{1 - e^{-\kappa h}}\right) + \ln(1 - e^{-2\kappa h})\right] \quad [6a]$$

$$\varphi_i = \frac{ze\phi_i}{k_B T} \quad [6b]$$

$$\kappa = \left(\frac{e^2 \Sigma n_{i\infty} z_i^2}{\epsilon\epsilon_0 k_B T}\right)^{1/2}, \quad [6c]$$

where n_∞ is the bulk number density of ions in solution, k_B is Boltzmann's constant, T is absolute temperature, φ_i is the reduced potential of either the collector or bacteria, ϕ_i is surface potential as determined by streaming potential or electrophoresis for the collector or bacteria, κ is the reciprocal Debye length, e is the charge of the electron, and z is the valence of an ion species. This expression was based upon a constant potential approximation and provided a lower bound for the predicted energy barriers (these barriers will increase upon incorporation of the constant charge approximation, as is the case in charge regulation models (26)). This equation was valid for systems with minimal electrical double-layer distortion ($\kappa a \gg 1$) where $h \ll a$ and for small surface potentials ϕ. Some error was anticipated within the Ottawa sand predictions because of the large negative zeta potential of the collector surface.

3. RESULTS

3.1. Surface Characterization of Interacting Surfaces

The streaming potential was used to determine zeta potential and charge stability of the four collectors. The preattritioning step showed clear signs that the iron (hydr)oxide was the least stable of the surface precipitates. Despite the higher losses of iron from the coated surfaces during preattritioning, the mixed (hydr)oxide and the aluminum (hydr)oxide coatings were determined to have positive zeta potentials of statistically different magnitudes. The loss of iron from the iron (hydr)oxide surface resulted in a net negative potential. Zeta potentials of all four collectors have been reported in Table 3. Streaming potential measurements on the granular material before and after the deposition experiments showed no changes in zeta potential. In addition, several supernatant samples from the deposition experiments were passed through a 0.25-micron filter and showed no presence of surface coating upon microscopic examination. Additional ICP analysis on the metal content for both the surface coating and the supernatant before and after the deposition experiments again showed no indication of coating loss during the deposition study.

FIG. 2. SEMEM iron map of Ottawa sand surface showing a region of patchwise surface impurity, a source of the surface charge heterogeneity, and a site for potentially favorable particle interactions (originally 680× magnification). Occurrence of these iron sites was intermittently observed on the surface.

Surface areas were also evaluated for the four collectors in order to rule out the possibility that any observed differences in bacterial deposition could be due to surface area availability. The results (Table 3) indicated that the coatings in fact decreased available surface area: Ottawa sand > mixed (hydr)oxide coating ≳ iron (hydr)oxide coating > aluminum (hydr)oxide coating. The loss of surface area upon coating did not appear to justify the observed depositional trends.

EDS was used in the preliminary evaluation of the Ottawa sand surface and indicated a presence of iron and aluminum impurities. No other substantial elemental quantities were observed within the Ottawa sand substrate. SEMEM analysis of the Ottawa sand surface indicated that naturally occurring aluminum deposits were uniformly distributed over the surface. The iron deposits were, however, found as patches on the surface (Fig. 2) in low occurrence. The SEMEM signal was determined not to be due to the topological character of the collector surfaces. Under further magnification, these

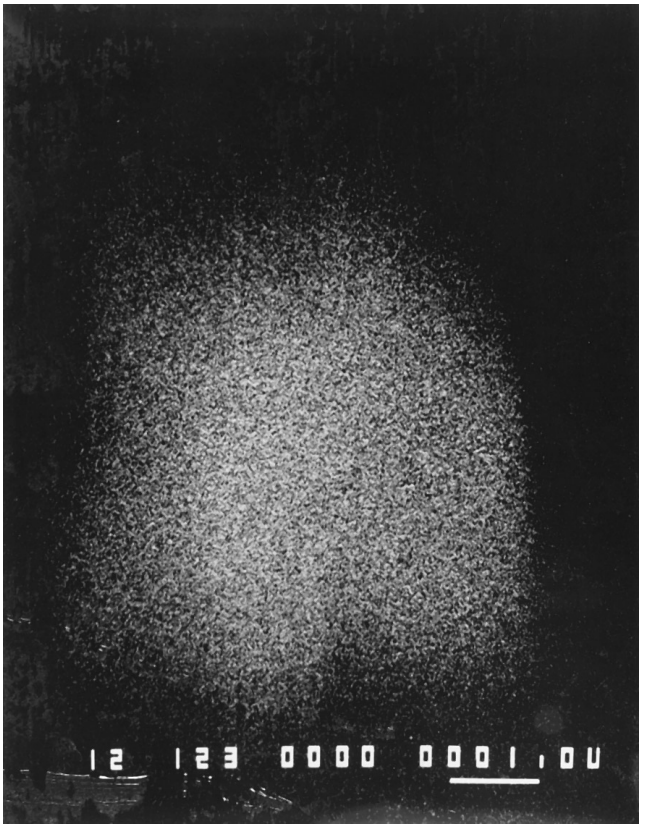

FIG. 3. SEMEM iron map of Ottawa sand surface emphasizing the size of these patchwise impurities to be much greater than the projecting area of the bacteria used in this study (originally 12,000× magnification).

FIG. 4. SEMEM aluminum map of an aluminum (hydr)oxide coated Ottawa sand surface showing the regularly observed patchwise surface impurities (originally 680× magnification). Micrograph was representative of entire surface.

patches of higher iron character were shown to be on the order of several square microns in area (Fig. 3) as compared to the 0.3 to 1.0 square micron areas of the microorganisms studied. The frequency of these metallic patches was observed to dramatically increase upon application of the metal (hydr)oxide coatings. A micrograph of an aluminum (hydr)oxide treated surface has been included as Fig. 4.

Electrophoresis was used to determine the zeta potential of the four bacterial species. The technique indicated that the zeta potentials of three of the four strains were statistically similar. The *S. typhimurium* was the exception of the four microbes and was found to have a weaker negative potential than the others (Table 1). Again, all zeta measurements were taken at pH 7.0 in order to correspond to the conditions used within the deposition studies.

3.2. Deposition Results

The bacterial deposition data was modeled as a first-order process (Eq. [3]) and characterized with corresponding first-order kinetic rate constants. The model was observed to adequately fit the deposition data as a function of time, and a few sample sets of data have been included as Fig. 5. The resulting kinetic rate constants, shown in Fig. 6, indicated a statistically significant increase in the removal of microbes for the metal (hydr)oxide surface coatings. The electropositive surfaces (aluminum and mixed iron/aluminum coatings) showed the largest kinetic rate constant values and

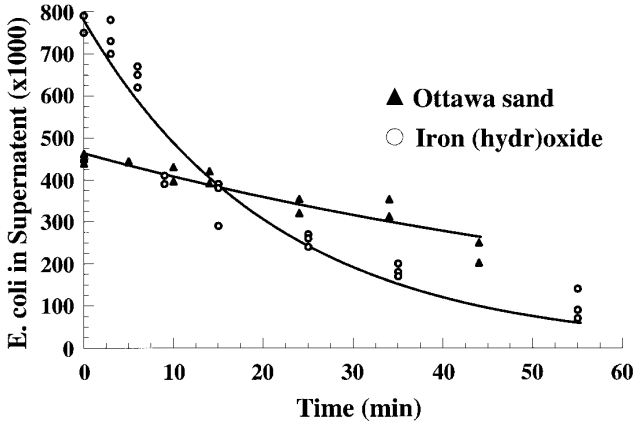

FIG. 5. Sample set of data representing *E. coli*–Ottawa sand (solid triangles) and *E. coli*–iron (hydr)oxide (open circles). This graph is intended to show the differences between a collector with a higher kinetic rate constant, iron ((hydr)oxide), and one with a low rate constant, Ottawa sand. All curves were fitted with an exponential curve using nonlinear least-squares regression.

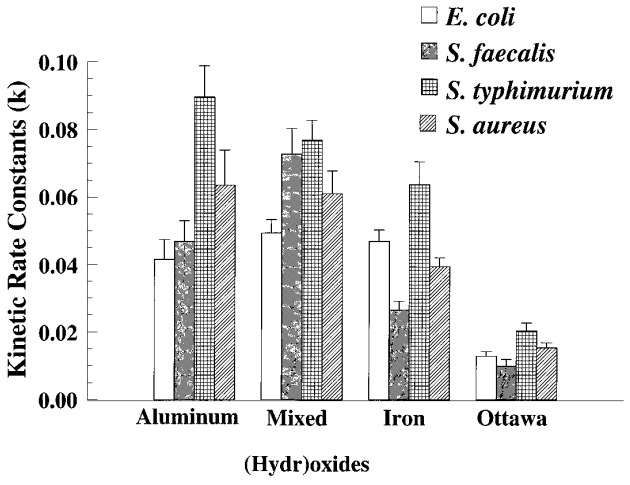

FIG. 6. Bar chart showing the kinetic rate constants of deposition of the four microbial species on the four collector surfaces. Values were determined from fitting an exponential model to the deposition data. The data has been presented as a function of the different metal (hydr)oxide coatings (labeled along the bottom axis). The reported uncertainties for the parameters are the standard errors from the regression analysis.

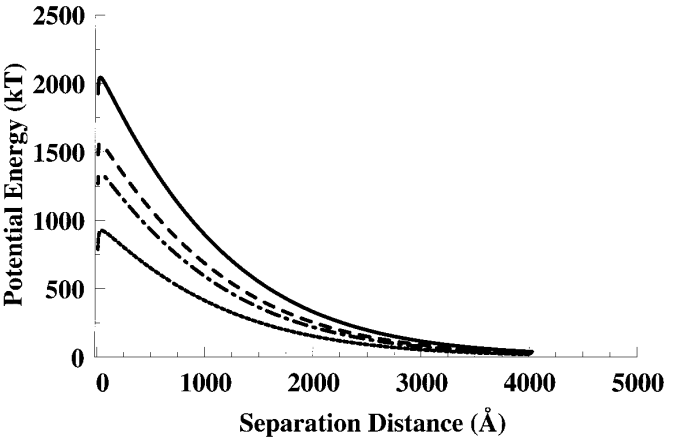

FIG. 7. Graphical representation of conservatively predicted DLVO energies as a function of particle separation and type of microbe for the iron (hydr)oxide coating. *E. coli* (solid line) shows the largest energy barrier, followed by *S. faecalis* (large-dashed line), then *S. aureus* (dash–dot line), and finally *S. typhimurium* (small-dashed line). The coated media had a surface potential of −50 mV.

indicated the highest deposition efficiency. In addition, the average kinetic rate constants observed for the aluminum (hydr)oxide and the mixed (hydr)oxide were statistically similar as $k = 0.0604 \pm 0.006$ min^{-1} and $k = 0.0650 \pm 0.006$ min^{-1}, respectively, suggesting bacterial deposition to be transport limited in the case of these two coatings. These two electropositive coatings had an average kinetic rate constant 1.5 times larger than what was observed for the iron (hydr)oxide coating and were 5 times larger than the rate constant values observed for the untreated Ottawa sand. Even the iron-coated medium with a zeta potential of −50 mV (40 mV more positive than the uncoated Ottawa sand) showed rate constants on the average 3.5 times greater than the constants seen for the Ottawa sand media.

3.3. DLVO Predictions

Systems of like charges, such as observed for Ottawa sand and iron (hydr)oxide deposition systems, were expected to have a large energy barrier as the rate-controlling step to particle attachment. For large energy barriers, the kinetic rate of particle attachment (k) was expected to decrease (19, 27). The DLVO predicted curves for the iron and Ottawa sand systems have been included in Figs. 7 and 8. These Helmholtz potential curves predicted very substantial energy barriers which should have prevented bacterial deposition. Deposition on the iron (hydr)oxide coating and Ottawa sand appeared to be somewhat inconsistent with this theoretical prediction based on detectable depositional rate constants for these two systems in spite of the resulting energy barriers on the order of several hundred to several thousand *kT*. Because the deposition rate was expected to decrease approximately exponentially with the height of the energy barrier over *kT*, it would have been very unlikely that the bacteria of this study would have had the necessary energy by thermal fluctuations to transverse the large predicted energy barriers. In addition, the theory as shown in Figs. 7 and 8 suggested that if the bacterial rate constants were influenced by double-layer and van der Waals forces, in spite of the large energy barriers, removal should follow the order *S. typhimurium* > *S. aureus* > *S. faecalis* > *E. coli*, in both the Ottawa sand and iron-coated systems. However, the measured rate constants for the iron and the Ottawa sand system followed the trend *S. typhimurium* > *E. coli* > *S. aureus* > *S. faecalis* (Fig. 6). This disagreement also suggested the

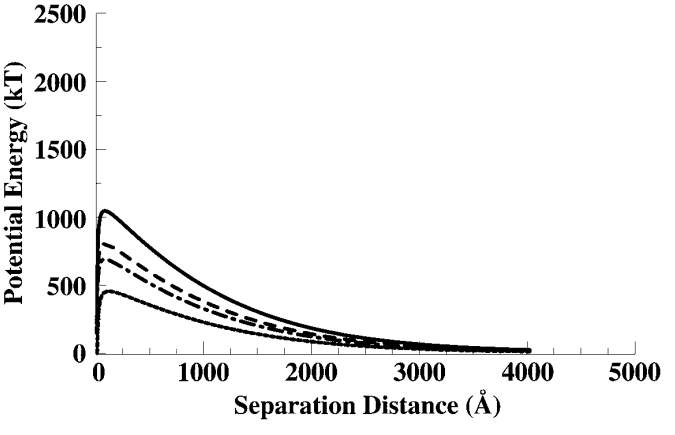

FIG. 8. Graphical representation of conservatively predicted DLVO energies as a function of particle separation and type of microbe for non-coated Ottawa sand. *E. coli* (solid line) shows the largest energy barrier, followed by *S. faecalis* (large-dashed line), then *S. aureus* (dash–dot line), and finally *S. typhimurium* (small-dashed line). The Ottawa sand had a surface potential of −90 mV.

importance of other non-DLVO parameters in bacterial deposition, particularly between the gram-negative and gram-positive microbial species.

DLVO theory, however, correctly predicted the qualitative deposition trend between the collector media. As expected, the collector surfaces with positive surface potentials (aluminum and mixed (hydr)oxides) removed more bacteria than the negative counterparts (iron (hydr)oxide and uncoated Ottawa sand).

4. DISCUSSION

For positively charged surfaces coated with mixed (hydr)oxide and aluminum (hydr)oxide coatings, DLVO theory predicted the absence of any energy barriers and transport-limited particle attachment (28). Figure 6 in fact suggested this behavior for the aluminum and mixed (hydr)oxides. A comparison of the average rate constants for bacterial deposition between the two positive collector surfaces showed that the aluminum (hydr)oxide and the mixed (hydr)oxide had similar depositional rate constant values, on average 1.5 times larger than what was observed for the iron (hydr)oxide coating and 5 times larger than the rate constants observed for the untreated Ottawa sand. These results suggested the possibility for substantial improvement of microbe capture through the removal of the interaction energy barrier between the particle and surface by removal of the double layer repulsion.

For negatively charged Ottawa sand and iron (hydr)oxide surfaces, the reduced deposition rate constants relative to those of the positively charged surfaces were consistent with DLVO theory as a result of the predicted energy barrier to attachment. However, significant bacterial deposition was observed within these negative systems, a fact not consistent with the very large energy barriers predicted by DLVO theory. The failure of the theory to predict microbial attachment kinetics has been reported by several other researchers for various systems (17, 18, 29, 30). Previous explanations of this observation have included deposition within a secondary minimum, influence of shape factors on particle interactions, interfacial dynamics of double-layer interactions, collector surface roughness, and distributions in surface potential (13). Of these theories, the most frequently cited explanation accounting for the deposition has been based upon surface nonidealities such as cracks, crevasses, and surface impurities on the granular medium (7, 31–34) which in turn have produced surface charge heterogeneities. The lower surface area recorded for the iron (hydr)oxide surface relative to the Ottawa sand surface suggested a decrease in surface nonidealities contrary to the increased deposition. Alternatively, the Ottawa sand was shown via EDS to have positive metal impurities of aluminum and iron on the surface. These metallic impurities could provide favorable sites for particle interaction if present as large patches on the Ottawa sand substrate. Further analysis of the Ottawa sand surface via SEMEM also supported the plausibility of this explanation accounting for the anomalous deposition. As shown in Figs. 2 and 3, iron (hydr)oxide deposits were found to be intermittently present on the Ottawa sand surface as patchwise heterogeneities with surface areas of several square microns, the projected area of interaction for a bacterium having been on the order of 0.3 to 1.0 square microns. SEMEM analysis also showed the aluminum to be randomly and more uniformly distributed on the surface. Since the streaming potential measurements indicated that the sand surface had a net negative potential, it would not seem likely that these disperse, uniform distributions of aluminum would have been responsible for producing the favorable sites for microbial deposition. Instead, the patchwise charge heterogeneities caused by the iron impurities would be the more probable sites for deposition within the Ottawa sand system.

The iron-(hydr)oxide-coated collector surface could also increase bacterial removal utilizing a similar mechanism. The preattritioning procedure, as outlined in the Materials and Methods section, resulted in a loss of the iron (hydr)oxide coating from the Ottawa sand surface. The resulting surface was found to have a net negative charge but appeared to be made up of discrete and random distributions of positively charged iron (hydr)oxide. The overall increased quantity of these positively charged patches relative to the Ottawa sand surface could account for the anomalous bacterial deposition in the iron system despite the existence of the large prohibitive energy barriers predicted by DLVO theory.

The deposition of bacteria onto the net positive collector surfaces would again be in response to the increased statistical probability that a bacterium would find itself in a region of the collector where the localized charge would correspond to an energy barrier less than 10 kT. Figure 4 shows a sample SEMEM micrograph of an aluminum-(hydr)oxide-coated surface demonstrating a clear increase in the number of sites available of lower interaction potential energy. The more continuous the aluminum (hydr)oxide or iron (hydr)oxide coatings, the higher the probability of particle capture. The results indicated that the rate of transport of the microbes to the positive collector surface governed the rate of particle capture on the aluminum (hydr)oxide and the mixed iron/aluminum (hydr)oxide collectors. The attachment event was correspondingly considered to be the rate-controlling step for the negative collector systems (Ottawa sand and mixed (hydr)oxides).

Although surface charge heterogeneity may have been the reason behind the bulk observed deposition of bacteria in general for negative collector systems, the removal trends between the bacterial species themselves deserved further consideration. For similarly charged systems of negative particles, the study failed to find a direct correlation between the depositional behavior of the individual microbes, Fig. 6, and the behavior predicted by the height of the energy barri-

ers calculated by DLVO theory, Figs. 7 and 8. This seemed to indicate that similarities in zeta potential, as seen for *S. faecalis, S. aureus,* and *E. coli,* had not correspondingly influenced the degree of microbial removal for systems of large energy barriers. In addition, the disagreement between the deposition trends of the diffusionally limited systems (aluminum (hydr)oxide and mixed (hydr)oxide) and the attachment limited systems (Ottawa sand and iron (hydr)oxide) suggested the possible importance of a misrepresentation of bacterial zeta potentials through surface conduction (25) or other non-DLVO parameters.

The kinetic deposition data indicated that the gram-negative bacteria (*S. typhimurium* and *E. coli*) were removed to a greater degree than the gram-positive bacteria in systems with negative collectors. One possible mechanism for the increase in particle attachment suggests the importance of bacterial surface appendages and their potential ability to contact the collector's surface and mediate bacterial attachment in spite of energy barriers. The length of flagella of these gram-negative bacteria typically range from 1 to 5 microns. In addition, fimbriae (pili) generally have a length between 0.3 and 1.0 microns (35). Such appendages could possibly traverse the predicted DLVO energy barriers of Figs. 7 and 8 while keeping the bacterial membrane at separation distances of 0.3 or 0.4 microns from the collector surface where the energy barriers would be minimal. Alternatively, these surface appendages may be able to probe along the collector surface and through their random motion find areas of favorable interaction where the energy barrier is less than 10 kT and the bacterial membrane can attach. Such an explanation could account for the particle capture through avoidance of the total height of the interaction energy barrier. Similarly, motility of the gram-negative microbes may also account for this deposition trend to some degree. The ability of the bacteria to move relative to the surface could increase each particle's likelihood of finding favorable sites for deposition. Such explanations would account for the apparent higher particle deposition for the gram-negative bacteria relative to the gram-positive.

5. SUMMARY

The purpose of this study was to quantitatively compare different metal (hydr)oxide coatings in enhancing bacterial deposition. Specifically, the deposition rates for bacterial strains *Streptococcus faecalis, Staphylococcus aureus, Salmonella typhimurium,* and *Escherichia coli* were compared for Ottawa sand and surface coatings consisting of aluminum (hydr)oxide, iron (hydr)oxide, and mixed iron and aluminum (hydr)oxide. The deposition results included within this paper have indicated that the metal (hydr)oxide surface coatings have the ability to increase bacterial deposition by up to a factor of 5 over that observed for untreated Ottawa sand. The results also seemed to indicate that the rate of transport of bacteria to the surface limited the net rate of deposition on the positive granular collectors largely independent of changes in the surface potential of the negative bacteria or the positive collector. Discrepancies between DLVO theory and the experimental deposition were observed, particularly with respect to bacterial deposition under situations of extremely large energy barriers as in the case of the Ottawa sand and the iron (hydr)oxide systems. These disagreements were probably due to the fact that macroscopic properties such as zeta potential were being used to predict interactions on a microscopic scale. Surface heterogeneity was the most probable reason for the unexpected deposition of both the gram-positive and gram-negative bacteria onto the negative collector surfaces in spite the large predicted energy barriers between particles. This would imply that bacterial attachment would be the rate-controlling step to particle deposition, and this would be a function of the distribution of the charge heterogeneity on the surface. Double-layer and van der Waals forces were the most probable key to the bulk bacterial deposition observed for all of these studies in granular media systems. This is not to say that the other aforementioned factors such as surface appendages, hydrophobicity, or surface roughness have little effect within the deposition process. The observed favored deposition of the gram-negative bacteria over the gram-positive bacteria under conditions governed by the particle attachment event suggests the importance of surface roughness, surface appendages, or bacterial motility as an area for further investigation.

ACKNOWLEDGMENTS

The authors would like to acknowledge the financial support of the Engineering Research Center (ERC) for Particle Science and Technology at the University of Florida, the National Science Foundation (NSF) grant # EEC-94-02989, and the Industrial Partners of the ERC. In addition, the authors wish to thank James Fitzgerald for his help with the SEMEM analysis, Josh Adler for the BET analysis, and Dr. Yongcheng Li for his helpful comments in the preparation of this manuscript.

REFERENCES

1. Murray, J. P., and Parks, G. A., *in* ''Particulates in Water'' (M. C. Kavanaugh and J. O. Leckie, Eds.), Adv. in Chem. Ser., Vol. **189,** pp. 97–133. American Chemical Society, Washington, D.C., 1980.
2. Farrah, S. R., and Preston, D. R., *Appl. Environ. Microbiol.* **50,** 1502–1504 (1985).
3. Rahner, S., Magaritz, M., and Amiel, A. J., *Appl. Geochem.* **n SUPPL 2,** 145–148 (1993).
4. Ahammed, M. M., and Chaudhuri, M., *J. Water SRT.* **45**(2), 67–71 (1996).
5. Lukasik, J., Farrah, S. R., Truesdail, S. E., and Shah, D. O., *Kona* **45**(1), 87–91 (1997).
6. Israelachvili, J., ''Intermolecular and Surface Forces.'' Academic Press, San Diego, 1992.
7. Elimelech, M., Gregory, J., Jia, X., and Williams, R. A., ''Particle Deposition and Aggregation.'' Butterworth-Heinemann, Boston, 1995.
8. Stenstrom, T. A., *Appl. Environ. Microbiol.* **55,** 142–147 (1989).

9. van Loosdrecht, M. C. M., Lyklema, J., Norde, W., Schraa, G., and Zehnder, A. J. B., *Appl. Environ. Microbiol.* **50**(8), 1898–1901 (1987).
10. van Loosdrecht, M. C. M., Lyklema, J., Norde, W., Schraa, G., and Zehnder, A. J. B., *Appl. Environ. Microbiol.* **53**(8), 1893–1897 (1987).
11. Gerba, C., Goyal, S. M., Cech, I., and Bogdan, G. F., *Environ. Sci. Technol.* **15,** 940–944 (1981).
12. Dickinson, R. B., *J. Colloid Interface Sci.* **190,** 142–151 (1997).
13. Elimelech, M., and O'Melia, C. R., *Langmuir* **6,** 1153–1163 (1990).
14. Kinoshita, T., Bales, R. C., Maguire, K. M., and Gerba, C. P., *J. Contam. Hydrol.* **14**(1), 55–70 (1993).
15. Kinoshita, T., Bales, R. C., Yahya, M., and Gerba, C. P., *Water Res.* **14**(8), 1295–1301 (1993).
16. Meinders, J. M., van der Mei, H. C., and Busscher, H. J., *J. Colloid Interface Sci.* **164**(2), 355–363 (1994).
17. Verwey, E., and Overbeek, J. Th. G., ''Theory of the Stability of Lyophobic Colloids.'' Elsevier, Amsterdam, 1948.
18. Derjaguin, B., and Landau, L., *Acta Physicochim. URSS* **14,** 733–762 (1941).
19. Prieve, D. C., and Ruckenstein, E., *J. Theor. Biol.* **56,** 205–228 (1976).
20. Parks, G. A., *Chem. Rev.* **65,** 177 (1965).
21. Hiemstra, T., Venema, P., and Van Riemsdijk, W. H., *J. Colloid Interface Sci.* **184,** 680–692 (1996).
22. Krarup, H. G., Linhart, R. V., and Adair, J. H., OPAL© for Windows$_{TM}$, Graphical Display of Hydrolysis Systems, Shareware, University of Florida, Materials Science and Engineering Department (1997), http://zirconia.mse.ufl.edu/opal.htm.
23. Bird, R. B., Stewart, W. E., and Lightfoot, E. N., ''Transport Phenomena.'' Wiley, New York, 1960.
24. Hiemenz, P. C., and Rajagopalan, R., ''Principles of Colloid and Surface Chemistry.'' Dekker, New York, 1997.
25. van der Wal, A., Minor, M., Norde, W., Zehnder, A. J. B., and Lyklema, J., *J. Colloid Interface Sci.* **186,** 71–79 (1997).
26. Grabbe, A., and Horn, R. G., *J. Colloid Interface Sci.* **157,** 375–383 (1993).
27. Li, Y., and Park, C. W., *J. Colloid Interface Sci.* **185,** 49–56 (1997).
28. Spielman, L. A., and Friedlander, S. K., *J. Colloid Interface Sci.* **46**(1), 22–31 (1973).
29. Gregory, J., and Wishart, A. J., *J. Colloid Interface Sci.* **1,** 313–334 (1980).
30. Johnson, P. R., Sun, N., and Elimelech, M., *Environ. Sci. Technol.* **30,** 3284–3293 (1996).
31. Song, L., Johnson, P. R., and Elimelech, M., *Environ. Sci. Technol.* **28,** 1164–1171 (1994).
32. Ryan, J. N., and Elimelech, M., *Colloids Surf. A* **107,** 1–56 (1996).
33. Holt, W. J. C., and Chan, D. Y. C., *Langmuir* **13,** 1577–1586 (1997).
34. Kapur, R., Lilien, J., Picciolo, G. L., and Black, J., *Bio. Mat. Res.* **32**(1), 133–142 (1996).
35. Freeman, A. B., ''Burrows Textbook of Microbiology,'' 21st ed. Saunders, Philadelphia, 1979.
36. Ross, S., and Morrison, I. D., ''Colloidal Systems and Interfaces.'' Wiley, New York, 1988.